Thermal rectification in silicon by a graded distribution of defects

Riccardo Dettori[1], Claudio Melis[1,2], Riccardo Rurali[3], Luciano Colombo[1,2,3,4*]

[1] *Dipartimento di Fisica, Università di Cagliari, Cittadella Universitaria, I-09042 Monserrato (Ca), Italy*

[2] *Istituto Officina dei Materiali, CNR-IOM SLACS Cagliari, Cittadella Universitaria, Monserrato (Ca) 09042-I, Italy*

[3] *Institut de Ciència de Materials de Barcelona (ICMAB-CSIC), Campus UAB, 08193 Bellaterra, Barcelona, Spain*

[4] *Catalan Institute of Nanoscience and Nanotechnology (ICN2), CSIC, and The Barcelona Institute of Nanoscience and Nanotechnology, Campus UAB, 08193 Bellaterra, Barcelona, Spain*

(Dated: May 18, 2016)

Abstract

We discuss computer experiments based on nonequilibrium molecular dynamics simulations providing evidence that thermal rectification can be obtained in bulk Si by a non–uniform distribution of defects. We consider a graded population of both Ge substitutional defects and nanovoids, distributed along the direction of an applied thermal bias, and predict a rectification factor comparable to what observed in other low–dimensional Si–based nanostructures. By considering several defect distribution profiles, thermal bias conditions, and sample sizes the present results suggest that a possible way for tuning thermal rectification is by defect engineering.

PACS numbers: 66.70.Df , 44.10.+i, 05.60.-k

*Corresponding Author: luciano.colombo@unica.it

I. INTRODUCTION

Thermal rectification [1–3] occurs whenever the heat flux is affected by the actual direction of the thermal gradient applied to the system. The amount of rectification of the heat current is usually quantified by the factor $R = |\vec{J}_{\rm fwd}|/|\vec{J}_{\rm rev}| - 1$, where $\vec{J}_{\rm fwd}$ and $\vec{J}_{\rm rev}$ are the heat flux corresponding to the forward and reverse thermal bias condition, respectively. The situation is conceptualized in Fig.1 for the prototypical configuration corresponding to an interface between two materials A and B. In Fig.1 we assumed that $\vec{J}_{\rm fwd} > \vec{J}_{\rm rev}$, but we remark that the definition of "forward" or "reverse" bias condition is just a matter of convention. While thermal rectification has been first observed experimentally long ago [4], recently it is attracting an increasing interest since it is a key feature in the emerging nanotechnology referred to as phononics [5–7]. Here the generation, control, and manipulation of lattice heat (or, equivalently, phonon flux) are the main tools to engineer devices with functionality similar to their electronic counterparts (like electrical diodes or transistors).

In most cases of practical interest [5] thermal rectification is observed when two materials with unlike thermal conduction properties are interfaced, as indeed shown in Fig.1. In this configuration, the role played by the sharp interface is crucial: here a temperature drop $\Delta T_{\rm fwd,rev}$ occurs in whatever bias condition, giving rise to an interface thermal resistance (ITR) quantified by the ratio $|\Delta T_{\rm fwd,rev}|/|\vec{J}_{\rm fwd,rev}|$ as extensively discussed in Refs.[2, 3, 8]. While ITR is largely referred to in semiconductor systems, also interfacial hybrid systems like metal/superconductor [9] or crystal/polymer [10] junctions have been shown to provide thermal rectification. However, the actual rectifying properties of an interface are affected by many features (structural details, chemical contamination, and interdiffusion to name just a few) which require non trivial nanofabrication techniques for their government, possibly resulting into a rather difficult technological task to be accomplished.

This scenario suggests that it would be interesting to observe thermal rectification without any localized (i.e. abrupt) temperature drop. This basically requires that such a sharp interface is not present in the rectifying device. Under this respect, low-dimensional systems (either model or realistic) prompt several possible rectifying configurations, like non-uniform mass loading, suited distributions of defects, and tailored shaping [11–17, 19, 20, 33] where the above combination is actually realized. In this work we further exploit this concept in bulk–like systems. In particular, by nonequilibrium molecular dynamics (NEMD) simula-

tions we address the thermal rectification factor R in Si bulk structures containing a gradual distribution of compositional or structural defects. The reason to select Si for the present investigation is twofold, namely: (i) it has impact in the emerging phononic nanotechnology quoted above, and (ii) it has very well-known thermal properties.

II. SIMULATION SETUP

NEMD simulations have been performed on Si tetragonal cells with section $S = n \times n\ a_0^2$ ($n = 10$ or 13, as indicated below) normal to the (001) direction of heat transport (hereafter named z) and a total length L_z varying in the range 100–350 a_0 (as indicated below). At the left and right extrema of such a simulation cell two further slabs of thickness 10 a_0 where added and coupled to thermostats (see below). Periodic boundary conditions have been applied along the two directions normal to z. We set $a_0 = 0.543$ nm as predicted by the Tersoff potential providing the force field for the present investigation [21]. The simulation cells have been at first filled by a diamond lattice of silicon atoms. Then, a non uniform dispersion of defects was obtained: (i) by randomly replacing Si atoms with Ge ones, up to a 20% of Ge content, which is the minimum doping corresponding to the maximum reduction of lattice thermal conductivity in a SiGe alloy [22, 23]; or (ii) by removing clusters of Si atoms so as to create voids with random position, size and shape up to a maximum 31% porosity. In any case the two thermostatted slabs were not affected by Si $\rightarrow$ Ge replacements or void generation. This procedure generated a defect distribution characterized by different concentration profiles along the z direction, as shown in Fig.2 (where the thermostatted slabs are not shown for sake of clarity). A structural relaxation followed, respectively, (i) through a careful energy minimization by conjugate gradients or (ii) through a high-temperature simulated annealing at 900 K. This latter procedure (implemented over 5×10^5 time steps of duration 0.5×10^{-15}s) was indeed required in order to allow for the full reconstruction of dangling bonds created by atom removals. In turn, the reconstruction generates a shell of amorphous matter at the void surface, providing an important source of phonon scattering in nanoporous Si [24]. In the case of a SiGe graded alloy, we also took care of any possible structural relaxation along the z direction due to the Si-Ge lattice mismatch by further performing constant-pressure, constant-temperature MD simulations as long as 5×10^5 time-steps, each lasting 1.5×10^{-15}s. Since we observed just a very minor variation of the cell

length and, in any case, no detectable effect in the calculation of the heat flux (see below), we present here results obtained with constant–volume cells. To this aim, fixed boundary conditions were imposed along z by adding on both sides one more plane where atomic positions have been clamped anytime during the simulations. Finally, for sake of comparison in both cases it has been generated a sharp interface between pure Si and, respectively, a homogeneous SiGe alloy with a 20% of Ge content or a nanoporous Si sample with 31% porosity.

The desired steady state thermal transport condition at which investigate possible rectification effects was generated in each system by coupling its left and right $10a_0$–thick terminal slabs (see above) to a heat reservoir, respectively set at $T_\mathrm{h} = 700$ K and $T_\mathrm{c} = 500$ K by using Nosé-Hoover thermostats. These temperature values guarantee that most part of the system stays above the Si Debye temperature and, therefore, quantum effects play a very minor role. While the initial temperature of each sample was set at the average $(T_\mathrm{h} + T_\mathrm{c})/2$ value, the MD simulation was aged until a steady state regime was reached for the selected thermal bias condition (assigned by the relative position of the hot and cold thermostats). Given the very small resulting thermal conductivity, this required as many 3×10^6 or 7×10^6 time steps of MD for the Ge-doped and nanoporous structures, respectively. In order to assess the steady state, we calculated both the work W_in and W_out, respectively spent by the hot and cold thermostat, and the corresponding heat fluxes $|\vec{J}_\mathrm{in,out}| = (1/S)(\partial W_\mathrm{in,out}/\partial t)$. A steady state condition was proclaimed only when $|\vec{J}_\mathrm{in}| = |\vec{J}_\mathrm{out}|$ to within the accepted numerical error (which we have set at 1%). This further required additional 1×10^6 or 3×10^6 time steps, according to the system. Once reached such a condition, the steady state heat flux for the assigned bias (i.e. $|\vec{J}_\mathrm{fwd}|$ or $|\vec{J}_\mathrm{rev}|$) was calculated as the average $(|\vec{J}_\mathrm{in}| + |\vec{J}_\mathrm{out}|)/2$. By inverting the two thermostats and repeating the calculation, the other heat flux was similarly calculated and the rectification R was eventually obtained. In all samples here investigated we named "forward" the bias condition where the pure silicon part of the system (i.e. the left end in Fig.2, all panels) was set at T_h. All simulations have been executed by using the `LAMMPS` code [25].

III. RESULTS AND DISCUSSION

Tab.I summarizes the results obtained for the configurations shown in Fig.2, reporting rectifications in the range 2.0-3.5 % and 1.4-3.2 % for Ge and pore distributions; on average the error in estimating rectification is about 0.45% and 0.32%, respectively. These data provide evidence that not only a rectification is indeed found, but also that it is ruled over by changing the distribution of Ge atoms or pores along the z direction. Overall the predicted R is comparable to what observed in other low-dimensional Si-based systems [26–31], proving that rectification is indeed possible in a bulk–like system missing of sharp interfaces. Interestingly enough, rectifications as small as 3-4% have been indeed measured in Si-based systems [32]; an even smaller rectification of about 1-2% has been experimentally reported, although in a rather different system as reduced graphene oxide [33]. So, the rectification values predicted in this work should be within the experimental capability of measure.

Varying the profile of the defect distribution is an effective way to control the resulting R and present simulations suggest that the exponential profile turns out to be the most efficient in generating different values for $|\vec{J}_{\rm fwd}|$ and $|\vec{J}_{\rm rev}|$. This is not, however, the only way to tune rectification features. In fact, we calculated the dependence of the rectification on the value of the imposed temperature offset $T_{\rm h} - T_{\rm c} = \Delta T$, as shown in Tab.II for the same $L_z = 100\ a_0$ sample containing a graded distribution of Ge defects with similar exponential profile. The results are along the expectations: by decreasing the temperature offset between the hot and cold thermostat the rectification is reduced from 3.5% to 2.7%. On average the error in estimating rectification for these systems is 0.37%. Interestingly enough, however, such a reduction is weak: while the temperature offset was reduced by a factor 4×, the calculated rectification is only reduced by a factor 1.3×. We believe this is an interesting results, making clear that the predicted rectification feature is robust. Interesting enough, the rectification is also affected by varying the absolute temperature of the two thermostats, but still preserving their offset: as a matter of fact, by repeating the calculation for an exponential profile of Ge substitutional defects with $T_{\rm h} = 900$ K and $T_{\rm c} = 700$ K we obtained $R = 4.3\%$. We attribute such an increased rectification to the different average interface temperature [34].

Another intriguing feature of the rectification phenomena here reported is that they are not paralleled by the onset of any interface temperature drop, possibly causing ITR

effects. Fig.3 reports the calculated temperature profiles in the steady state conditions for all graded systems shown in Fig.2, both in the forward (open blue symbols) and reverse (red full symbols) thermal bias condition. The profiles have been obtained by calculating the local temperature of slabs as thin as 2.7 nm aligned along the z direction, over which the atomic velocities have been averaged for 1×10^6 and 3×10^6 time steps, according to the system.

We fathom the present results in terms of a non–separable dependence of the thermal conductivity upon the z–coordinate and temperature T which, in turn, defines a non–linear heat transfer regime. Such a non–linear regime is the key feature for rectification, which cannot be simply ascribed to an asymmetric scattering of the heat carriers by defects when inverting the thermal bias. As a matter of fact, the structural inhomogeneity generated by the graded distribution of compositional or structural defects makes the thermal conductivity a function of z. On the other hand, it turns out that the same quantity is explicitly a function of T as well, since the system is out of equilibrium (although in steady state). In other words, we take for granted that each single portion of the system is transmitting heat while experiencing a local temperature different with respect to the temperature of its neighbouring regions. This is tantamount to say that in all investigated samples the function $\kappa = \kappa(z, T)$ is non–separable. Let us now assume that, contrary to the above conclusion, the thermal conductivity is separable, i.e. that we can write $\kappa(z, T) = f(z)g(T)$, where $f(z)$ and $g(T)$ are known function. In the steady state condition (whatever thermal bias) here investigated, the heat equation for one-dimensional transport along the z direction

$$\kappa(z, T)\frac{dT}{dz} = f(z)g(T)\frac{dT}{dz} = -J_z \tag{1}$$

can be easily integrated by variable separation since the one-dimensional heat flux J_z is a constant and, therefore, we get

$$\int_{T_\mathrm{l}}^{T_\mathrm{r}} g(T)dT = -J_z \int_{z_\mathrm{l}}^{z_\mathrm{r}} \frac{1}{f(z)}dz \tag{2}$$

where T_l and T_r are the temperature of left and right terminal ends of the system, respectively located at position z_l and z_r. Equivalently, eq.(2) can be cast in the form

$$J_z = -\frac{\int_{T_\mathrm{l}}^{T_\mathrm{r}} g(T)dT}{\int_{z_\mathrm{l}}^{z_\mathrm{r}} \frac{1}{f(z)}dz} \tag{3}$$

By inverting the thermal bias condition we just overturn the upper and lower limit in the temperature integral: this will only affect the sign of the heat flux, leaving unaffected its absolute value. This implies a null rectification, i.e. $R = 0$ since $|\vec{J}_{\rm fwd}| = |\vec{J}_{\rm rev}|$. Therefore, the assumption that $k(z,T) = f(z)g(T)$ is separable has in fact defined a *sufficient condition for no rectification* [35].

This is the key concept that allows to understand our results, providing a rationale for them. Sure enough, we can logically invert the above statement and say that a non separable $\kappa = \kappa(z,T)$ form of the thermal conductivity does represent the *necessary condition for rectification*. This is precisely what is exploited by the combination of (i) a graded distribution of defects and (ii) a thermal bias condition. Therefore, the bulk structures here investigate *must rectify* a thermal current: as a matter of fact, their thermal conductivity is a complicated and non–linear convolution given by a z–dependence of the temperature which, in turn, is a function of the local stoichiometry or porosity.

The present picture on rectification is robust since it does not qualitatively depend neither on the nature of the defects (compositional or structural) distributed in the bulk structure, nor on their actual distribution profile. It is also found for no matter what thermostatting condition is set: by simulating a graded exponential distribution of Ge defects under two different conditions (namely: $T_{\rm h} = 700$ K with $T_{\rm c} = 500$ K, and $T_{\rm h} = 900$ K with $T_{\rm c} = 700$ K) in both forward and reverse bias a smooth continuous temperature profile was found throughout the all sample, similarly to what shown in Fig.3.

When the same analysis is applied to the systems characterized by a step-like distribution of defects (Fig.2, bottom panels) we have indeed found a small (but definitely non-vanishing) and abrupt temperature offset at the interface, as reported in Fig.4. In the case of Ge doping, we evaluated such an interface temperature drop as large as $\Delta T_{\rm fwd} = 18.1 \pm 2.3$ K and $\Delta T_{\rm rev} = 21.6 \pm 2.6$ K for the forward and reverse bias situation, respectively. Similarly, for a step-like distribution of pores we calculated $\Delta T_{\rm fwd} = 11.9 \pm 4.2$ K and $\Delta T_{\rm rev} = 17.8 \pm 3.0$ K, resulting in a more relevant difference between the two thermal bias conditions.

We now turn to investigate another important issue, namely: how the predicted rectification is affected by the gradient of the defect distribution. To this aim, we have once again selected an exponential profile of Ge substitutional defects which, as in the previous cases, was varied from the minimum 0% to the maximum 20% content over a sample length L_z. However, in this case we considered four different samples with increasing thickness along the

direction of heat transport corresponding to $L_z = 100,\ 200,\ 300,\ 350\ a_0$, respectively. The resulting defect profiles are shown in Fig. 5. The two largest increased lengths correspond to quite a big simulation cell and, therefore, in order to keep sustainable the corresponding computational workload we reduced the sample cross section to $10 \times 10\ a_0^2$. This reduction makes unfair the direct comparison with the previously investigated sample with same L_z but larger S and, therefore, we recalculated the rectification for the new section. Results are shown in Tab.III, indicating that the rectification is predicted to decrease from 4.3% ($L_z = 100\ a_0$) to 3.3% ($L_z = 350\ a_0$), i.e. a 3.5× increase of the sample length has reduced rectification by only a factor 1.3×. On average the error in estimating rectification is 0.75%. So, as expected, there is indeed a reduction of the rectification features, but even in this case the dependence on the sample length is weak.

It is hard to assess whether this reduction is due to the increased (because of the increased sample length) scattering of heat carriers or, rather, to the decreased gradient in the defect distribution. In order to further substantiate the argument that the interplay between the sample length and the gradient of the defect distribution is complex, we considered one more configuration with $S = 13 \times 13\ a_0^2$, $L_z = 100\ a_0$ and an exponential profile of Ge substitutional defects which, however, was now varied from 0% to 60% of Ge-content. Interestingly enough in this case we found a smaller rectification than reported in Tab.I, a value in fact very similar to the rectification calculated for the step–like profile. A systematic set of simulations exploring various combinations of length and gradient effects would be needed to fully clarify this issue. We leave them to a following investigation.

Finally, by increasing the maximum Ge content of the doped region up to 60%, or by enlarging the $(T_\mathrm{h} - T_\mathrm{c})$ difference up to 400K, or even by reducing the thermostats temperature to $T_\mathrm{h} = 400$ K and $T_\mathrm{c} = 200$ K (and neglecting possible quantum effects), we have found full confirmation of the picture outlined above, namely: rectification up to $\sim 5\%$ is always observed in graded bulk structures without any ITR (once again, because of the missing sharp temperature drop anywhere in the system).

IV. CONCLUSIONS

In conclusion, we have shown that thermal rectification can be obtained in a bulk–like silicon system missing of any interface by exploring two different configurations where a

graded distribution of Ge substitutional defects or nanovoids, respectively, is arranged along the direction of an applied thermal gradient. This result is nicely consistent with the general argument that rectification is necessarily generated in any system where the thermal conductivity is a non–separable function of both temperature and position [35], indeed a situation found in any structure here investigated. For both graded distributions, we proved that rectification is obtained still preserving a very smooth temperature profile throughout the system, i.e. without setting up any localized temperature drop. Furthermore, it is found that the resulting value of R depends on the structural features of the graded distribution, as well as on the applied thermal bias and the actual gradient of the defect distribution. This, in turn, suggests a possible way for tuning thermal rectification by defect engineering. Finally, we remark that for any system here investigated the predicted R is comparable with the rectification observed in low–dimensional Si-based systems and lies within the experimental resolution.

Acknowledgments

We acknowledge financial support by the Spanish MINECO under grants no. FEDER-FIS2012-37549-C05-02, FEDER-MAT2013-40581-P, TEC2012-31330 and TEC2015-67462-C2-1-R, the Generalitat de Catalunya under grants no. 2014 SGR 301 and 2014 SGR 384, and the Spanish MINECO through the Severo Ochoa Centres of Excellence Program under Grants SEV-2013-0295 and SEV-2015-0496.

We also acknowledge financial support by the Regione Sardegna basic research project CRP78744 "Energy Applications with Porous Silicon (ENAPSi)"

One of us (R.D.) acknowledges Regione Sardegna for financial support under project P.O.R. Sardegna F.S.E. 2007-2013 (Axis IV Human Resources, Objective l.3, Line of Activity l.3.1.).

We finally acknowledge computational support by CINECA under ISCRA project `TREWI`.

[1] B. Li, L. Wang, and G. Casati, Phys. Rev. Lett. **93**, 184301 (2004).

[2] N.A. Roberts and D.G. Walker, Int. J. Therm. Sci. **50**, 648 (2011).

[3] C. Dames, J. Heat Transfer **131**, 061301 (2009).

[4] C. Starr, J. Appl. Phys. **7**, 15 (1935).

[5] D.G. Cahill, P.V. Braun, G. Chen, D.R. Clarke, S. Fan, K. E. Goodson, P. Keblinski, W.P. King, G.D. Mahan, A. Majumdar, H.J. Maris, S.R. Phillpot, E. Pop, and L. Shi, Appl. Phys. Rev. **1**, 011305 (2014).

[6] N. Li, J. Ren, L. Wang, G. Zhang, P. Hänggi, and B. Li, Rev. Mod. Phys. **84**, 1045 (2012).

[7] S. Volz, J. Ordonez-Miranda, A. Shchepetov, M. Prunnila, J. Ahopelto, T. Pezerilc, G. Vaudel, V. Gusevd, P. Ruello, E.M. Weige, M. Schubert, M. Hettich, M. Grossman, T. Dekorsy, F. Alzina, B. Graczykowsky, E. Chavez-Angel, J.S. Reparaz, C.M. Sotomayor-Torres, S. Xiong, S. Neogih, and D. Donadio, Eur. Phys. J. **89**, 15 (2016).

[8] E.T. Swartz and R.O. Pohl, Rev. Mod. Phys. **61**, 605 (1989).

[9] M.J. Martıńez-Pérez, A. Fornieri, and F. Giazotto, Nature Nanotch. **10**, 303 (2015).

[10] M. Hu, P. Keblinski, and B. Li, Appl. Phys. Lett. **92**, 211908 (2008).

[11] N. Yang, N. Li, L. Wang, and B. Li, Phys. Rev. B **76**, 020301(R) (2007).

[12] R. Rurali, X. Cartoixà, and L. Colombo, Phys. Rev. B **90**, 041408(R) (2014).

[13] X. Cartoixà, L. Colombo, and R. Rurali, Nano Letters, **15**, 8255 (2015).

[14] C.W. Chang, D. Okawa, A. Majumdar, and A. Zettl, Science **314**, 1121 (2006).

[15] G. Wu and B. Li, J. Phys.: Condens. Matter **20**, 175211 (2008).

[16] N. Yang, G. Zhang, and B. Li, Appl. Phys. Lett. **93**, 24311 (2008).

[17] J. Hu, X. Ruan, and Y.P. Chen, Nano Letters **9**, 2730 (2009).

[18] H. Tian, D. Xie, Y. Yang, T.-L. Ren, G. Zhang, Y.-F. Wang, C.-J. Zhou, P.-G. Peng, L.-G. Wang, and L.-T. Liu, Sci. Reports, **2**, 523 (2012).

[19] L. Medrano Sandonas, R. Gutierrez, A. Dianatac and G. Cuniberti, RCS Adv. **5**, 54345 (2015).

[20] C. Melis, G. Barbarino, and L. Colombo, Phys. Bev. B **92**, 245408 (2015).

[21] J. Tersoff, Phys. Rev. B **39**, 5566 (1989).

[22] J. Garg, N. Bonini, B. Kozinsky, and N. Marzari, Phys. Rev. Lett. **106**, 045901 (2011).

[23] C. Melis and L. Colombo, Phys. Rev. Lett. **112**, 065901 (2014).

[24] R. Dettori, C. Melis, Xavier Cartoixá, R. Rurali, and L. Colombo, Phys. Rev. B **91**, 054305 (2015).

[25] S. Plimpton, J. Comp. Phys. **117**, 1 (1995). See also the following site: `http://lammps.sandia.gov`.

[26] X. Zhang, M. Hu, and D. Tang, J. Appl. Phys. **113**, 194307 (2013).

[27] M. Schmotz, J. Maier, E. Scheer and P. Leiderer, New J. Phys. **13**, 113027 (2011)

[28] B.L. Geist, M. Zaynetdinov, K. Myers, H.D. Robinson, and V. Kochergin, MRS Proceedings, **1735** (2015), doi:10.1557/opl.2015.272.

[29] S. Ju and X. Liang, J. Appl. Phys. **112**, 024307 (2012).

[30] S. Ju and X. Liang, J. Appl. Phys. **112**, 054312 (2012).

[31] M. Criado-Sancho, F. X. Alvarez, and D. Jou, J. Appl. Phys. **114**, 053512 (2013).

[32] C.W. Chang, D. Okawa, A. Majumdar, and A. Zettl, Science **314**, 1121 (2006).

[33] H. Tian, D. Xie, Y. Yang, T.-L. Ren, G. Zhang, Y.-F. Wang, C.-J. Zhou, P.-G. Peng, L.-G. Wang, and L.-T. Liu, Sci. Reports **2**, 523 (2012).

[34] R. Rurali, L. Colombo, X. Cartoixà, Ø. Wilhelmsen, T.T. Trinh, D. Bedeaux, and S. Kjelstrup, Phys. Chem. Chem. Phys. **18**, 13741 (2016).

[35] D.B. Go and M. Sen, J. Heat Transfer **132**, 124502 (2010).

Table I: Rectification calculated for the graded distributions of Ge atoms or pores shown in Fig.2. On average the error in estimating rectification is about 0.45% and 0.32%, respectively. For all samples the temperature offset between the hot and cold thermostat is set at $\Delta T = 200$ K and it is centred at an average temperature of 600 K. Simulation cells have a $13 \times 13\ a_0^2$ section and a length $L_z = 100\ a_0$.

	linear	quadratic	exponential	step-like
Ge	2.0%	2.8%	3.5%	2.0%
pores	1.6%	1.4%	3.2%	1.2%

Table II: Rectification calculated for a graded distributions of Ge atoms with an exponential profile (see Fig.2) as function of the temperature offset ΔT between the hot and cold thermostat (in all cases the average temperature is 600 K). On average the error in estimating rectification is 0.37%. The simulation cells have a section $S = 13\times\ 13\ a_0^2$ and a length $L_z = 100\ a_0$.

$\Delta T = 200$ K	$\Delta T = 150$ K	$\Delta T = 100$ K	$\Delta T = 50$ K
3.5%	3.3%	2.8%	2.7%

Table III: Rectification calculated for a graded distributions of Ge atoms with an exponential profile (see Fig.2) as function of the length L_z of the simulation cell. On average the error in estimating rectification is 0.75%. In this case the cross section was reduced to $10 \times 10\ a_0^2$ for computational convenience. The temperature offset between the hot and cold thermostat is set at $\Delta T = 200$ K and centred at an average temperature of 600 K.

$L_z = 100\ a_0$	$L_z = 200\ a_0$	$L_z = 300\ a_0$	$L_z = 350\ a_0$
4.3%	4.1%	3.6%	3.3%

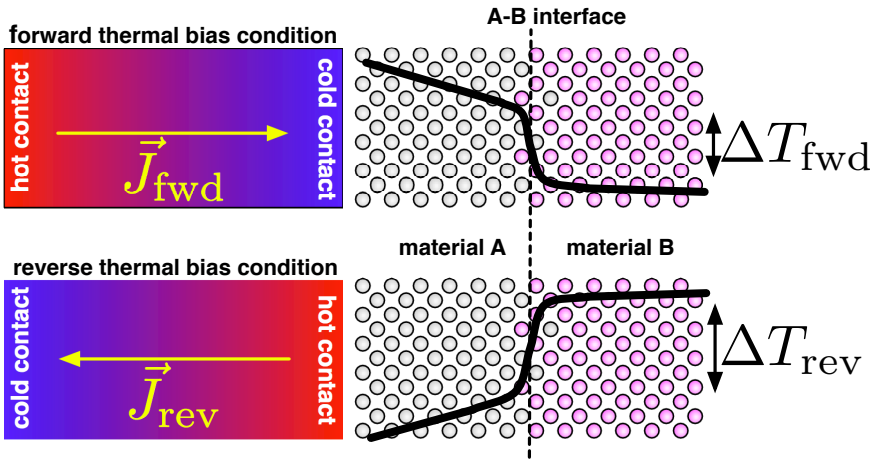

Figure 1: (color online) Left: schematic representation of the "forward" and "reverse" thermal bias conditions. Rectification occurs whenever $\vec{J}_{\rm fwd} \neq \vec{J}_{\rm rev}$. Right: zoomed interface region where the temperature drop ΔT occurs (full black line), generating localized thermal resistance.

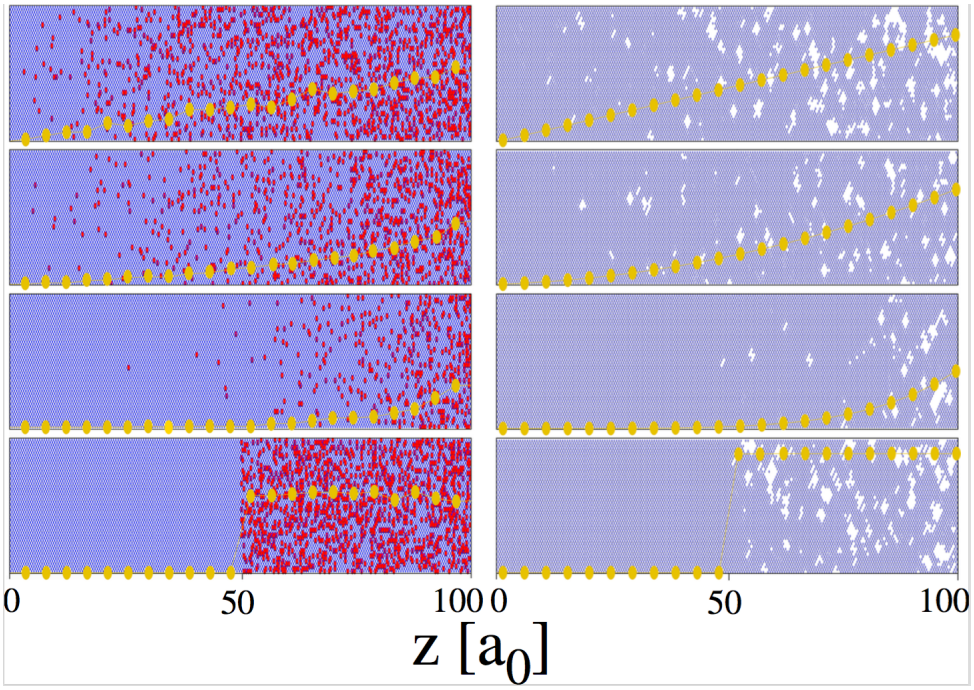

Figure 2: (color online) Graded distribution of substitutional Ge defects (left) and pores (right) in a Si lattice (light blue). From top to bottom it is shown a linear, quadratic, exponential, and step-like distribution of defects. Their average concentration is shown by a yellow dot-line. Pictures show a $4a_0$-thick longitudinal section of each sample.

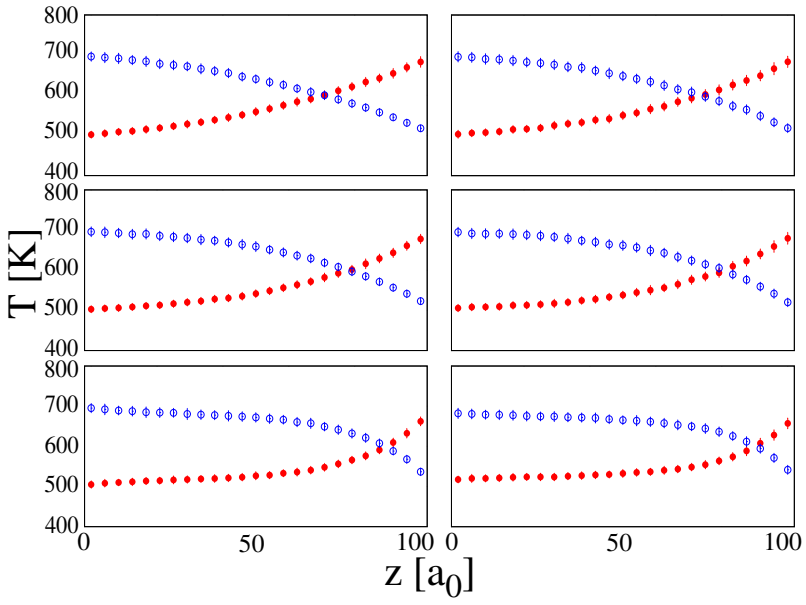

Figure 3: (color online) Temperature profiles calculated for the graded distributions of Ge atoms (left) and pores (right) shown in the same order of Fig.2 (the step-like profile is here omitted for sake of clarity). For all systems it has been set $T_{\rm h} = 700$ K and $T_{\rm c} = 500$ K. The forward and reverse thermal bias conditions correspond to the empty (blue) and full (red) symbols, respectively. Errors are indicated by vertical bars.

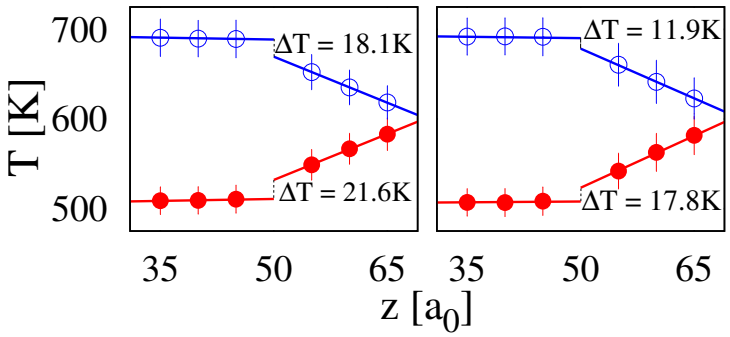

Figure 4: (color online) Zoomed temperature profiles nearby the interface (positioned at $z = 50$ a_0) calculated for a step-like distribution of Ge atoms (left) and pores (right) in the $T_h = 700$ K and $T_c = 500$ K thermostatting condition. The resulting temperature drop ΔT is shown for both the forward (empty blue symbols) and reverse (full red symbols) thermal bias conditions. Errors are indicated by vertical bars.

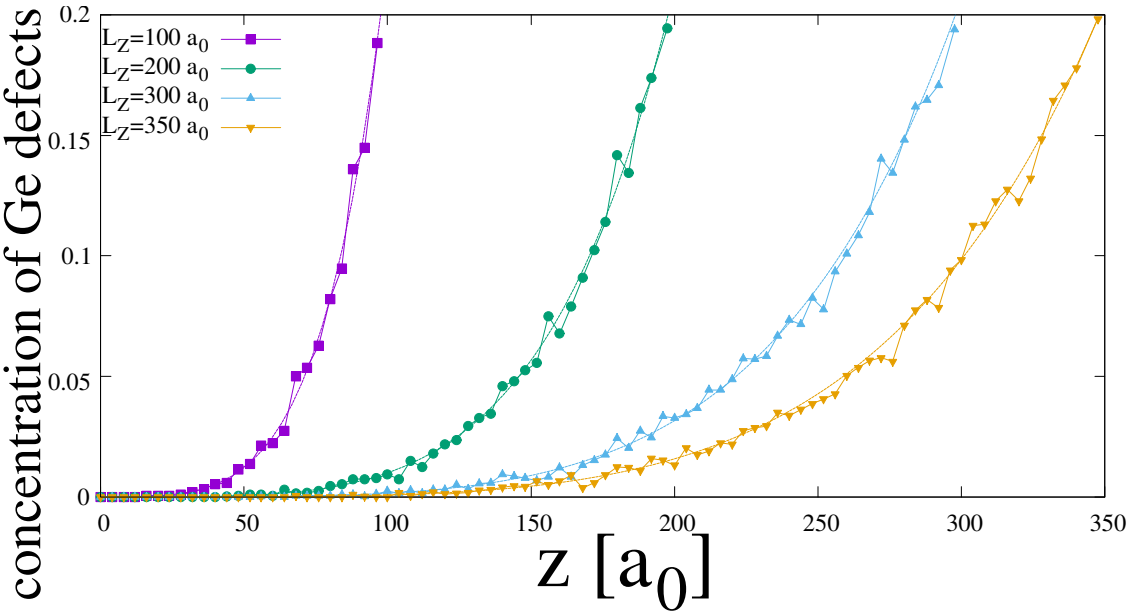

Figure 5: (color online) Local content of Ge substitutional defects along the direction z of heat transport for four samples with different length L_z. Symbols (connected by thick lines) represent the actual Ge content; thin lines represent a guide to the eye, corresponding to an ideal exponential profile.